

UNCERTAINTY QUANTIFICATION ON MULTISCALE MODELING OF RRAM DEVICES

Ziyan Liao¹, Zhiheng Huang^{1*}, Min Xiao¹, Yuezhong Meng¹, Hui Yan² and Yang Liu³

¹ The Key Laboratory of Low-carbon Chemistry & Energy Conservation of Guangdong Province, and School of Materials Science and Engineering, Sun Yat-sen University, Guangzhou, China

² School of Computer Science and Engineering, Sun Yat-sen University, Guangzhou, China

³ School of Electronics and Information Technology, Sun Yat-sen University, Guangzhou, China

*Corresponding Author's Email: hzh29@mail.sysu.edu.cn

ABSTRACT

This work employs the uncertainty quantification method to systematically analyze the power consumption and forming voltage in RRAM devices, emphasizing the significant role of material factors in multiscale and multiphysics processes. The uncertainty quantification approach drives a macroscopic-scale thermoelectric model to simulate RRAM switching and identifies key parameters. Furthermore, the same approach is adopted to control a mesoscale phase-field model that simulates the kinetics of conductive filament evolution. The results of the two models complement each other and provide a better understanding of the dynamics occurring inside the RRAM device and the origin of the performance uncertainty.

INTRODUCTION

Resistive Random Access Memory (RRAM) is a nonvolatile memory that operates by switching resistance between the formation and the rupture of the conductive filament (CF), corresponding to the binary states of '0' and '1'. RRAM is regarded as the leading contender for future memory technologies, due to its compelling features such as high storage capacity, fast write-read speed, low power consumption, and excellent scalability [1]. However, the uncertainty of the microstructure in the materials and microprocesses occurring in the device makes the control of RRAM a challenging task. Therefore, an Integrated Computational Materials Engineering (ICME) approach is desirable and essential to systematically examine the behavior of RRAM by considering multiscale microstructures and multiphysics processes. In addition, incorporating uncertainty quantification (UQ) analysis into the ICME framework can enhance its ability to address uncertainty in RRAM devices. Here, two models of different scales are introduced, i.e., a model at the macroscopic scale with coupled thermal and electrical physics based on finite element analysis (hereafter referred to as FE model) and a mesoscopic scale phase-field (PF) model, and the UQ method are used to systematically explore the influence of uncertainties from material factors on the performance of RRAM devices.

MODELS AND UQ METHODS

The FE model is based on TiN/Hf/HfO_{2x}/TiN RRAM proposed by Niraula *et al.* [2]. The power consumption of the model is selected as the quantity of interest (QoI) to perform the UQ analysis. The model consists of four distinct yet seamlessly integrated modules, corresponding to the ON and OFF states and the SET (OFF→ON) and RESET (ON→OFF) switching processes. The mechanism of switching in this model is primarily driven by thermodynamics, which involves controlled manipulation of the voltage, pulse amplitude, and polarity, with contributions from electrostatic, thermal, and chemical free energies.

A PF model can further explore the impact of fundamental material parameters on RRAM performance at the mesoscale. The PF model simulates the complete switching process of RRAM, consisting of the ON, OFF, SET, RESET processes, and includes an additional forming process that is not present in the FE model. The same UQ analysis is also performed on the PF model. Based on the Kim-Kim-Suzuki (KKS) model [3], and the electrochemical processes models developed by Shibuta *et al.* [4], a consistent PF model can be assembled in the integrated MATLAB-COMSOL Multiphysics modeling platform to simulate RRAM switching cycles and derive I-V characteristics. A continuous PF order parameter ϕ represents the transition and evolution between the HfO₂ matrix phase (α) and the CF phase (β) in RRAM. By solving for the order parameter ϕ over time and space, the kinetics of the evolution of the CF can be obtained.

UQ methods are crucial for assessing and managing uncertainties in models. The Morris One At a Time (MOAT) screening method [5] involves the use of factorial sampling plans to identify important inputs by evaluating the elementary effects of each parameter. Sensitivity analysis uses Sobol indices (SI) to quantify contributions from individual inputs or their combinations [6]. The first-order SI isolates the effect of a single input, while the total SI encompasses all contributions. Uncertainty propagation estimates the model's probability density function (PDF) from input distributions, using kernel density estimation (KDE) to infer the shape of PDF [7]. Reliability analysis is used to calculate the probability that QoIs meet specific conditions, using Monte Carlo

sampling to approximate the integral of the region where these conditions are met [8].

RESULTS AND DISCUSSION

Predicted I-V curves from the models

The FE model takes into account the thermodynamic processes by minimizing the free energy and simulates the complete switching process of RRAM at the macroscopic scale. The predicted I-V curve is presented in Fig. 1. The O-A segment represents the OFF stage, where the voltage increases with a 100 V/s ramp rate. When the voltage reaches point A, the device enters the SET process defined by the B-C segment, during which a stable CF radius is calculated by minimizing the free energy. As the voltage drops to 0 and then increases in the reverse direction, the device switches to the ON stage, represented by the C-O-D segment. Subsequently, the device enters the RESET process defined by the E-F segment, during which the CF breaks. Finally, the voltage returns to 0, and the device reverts to the OFF stage, corresponding to the F-O segment.

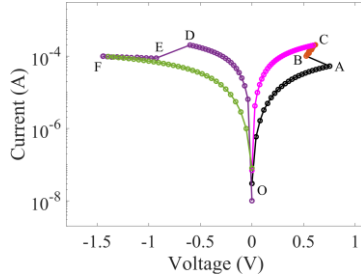


Figure 1: An example I-V curve for a complete switching cycle of RRAM predicted by the FE model

Although the FE model mentioned above incorporates a thermodynamic analysis, the microstructural morphology of the CF and its evolution during the processes of formation and rupture should be carefully examined, as the microstructural information can be the origin of the performance uncertainty of RRAM devices. The PF model simulates the same switching cycle as the FE model, with an additional consideration on a forming process. Furthermore, because of a difference in the focused length scale, the parameters in both models cannot be set entirely consistent. By solving the Poisson's equation for the electric potential distribution, the diffusion equation of oxygen vacancies, and the phase field evolution equation, the morphological evolution of the CF is obtained, and the I-V curve of RRAM can be derived, as shown in Fig. 2(a). Under a positive voltage, oxygen ions migrate into the electrode, leaving oxygen vacancies in α phase to form the CF, and connecting the two electrodes, as shown in Fig. 2(b). Under reverse voltage, oxygen ions migrate back into the α phase and combine with oxygen vacancies, causing partial rupture of the CF, and switching the device to the RESET process, as shown in Fig. 2(c). Reapplying a positive voltage allows the CF to grow again and the cycle repeats.

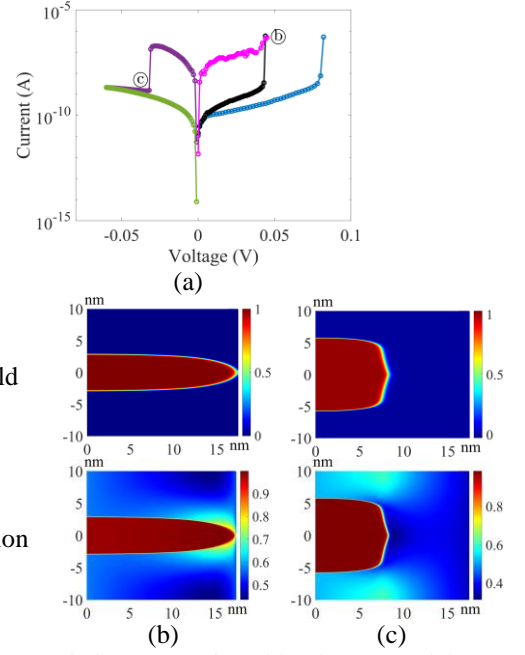


Figure 2: RRAM behavior predicted by the PF model: (a) an exemplar I-V curve for a complete switching cycle, the morphological evolution of the CF phase and the composition of the oxygen vacancies in (b) SET and (c) RESET process

UQ on power consumption

The power consumptions in the SET and RESET processes are defined as P_{set} and P_{reset} , respectively, and other key parameters are listed below in Table I.

TABLE I. A LIST OF KEY PARAMETERS

Parameter	Physical meaning
σ	Electrical conductivity
κ	Thermal conductivity
α_{fil}	A constant of σ_{CF}
h	The thickness of oxide layer
R_L	Load resistance
D	Diffusivity
λ	The interface thickness
M_ϕ	The phase field mobility
R	The nucleation radius
γ	The interfacial energy

Fig. 3 presents the results of the MOAT screening in the FE model. Fig. 3(a) shows the relative importance of different parameters affecting P_{set} , with α_{fil} being the most significant due to its highest mean and standard deviation, and σ_{CF} ranking the second most influential. Similarly, Fig. 3(b) provides valuable insight into the parameters affecting P_{reset} . σ_{CF} has the highest mean, indicating a noticeable impact on P_{reset} , while α_{fil} , h and R_L exhibit higher standard deviations, suggesting nonlinear effects or interactions among these parameters. The results indicate that P_{set} can be reduced by 32% with the following parameter setting: $\alpha_{\text{fil}} = -0.07$, $\sigma_{\text{CF}} = 10^5$ S/m, $h = 9$ nm and $\kappa_{\text{SiO}_2} = 1.5$ W/(m·K), and

the reliability analysis indicates a probability of 0.158 for this improvement. Moreover, P_{reset} can be reduced by 38% with the following parameter setting: $\alpha_{\text{fil}} = -0.07$, $\sigma_{\text{CF}} = 10^5 \text{ S/m}$, $h = 3 \text{ nm}$ and $R_L = 3.5 \text{ k}\Omega$, and the reliability analysis reveals a probability of 0.186 for this improvement.

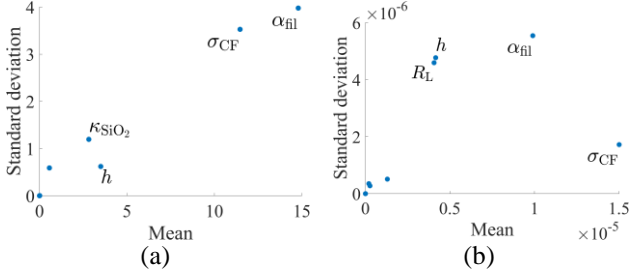


Figure 3: The results of the MOAT screening on (a) P_{set} and (b) P_{reset} in the FE model

Fig. 4 shows the results of the sensitivity analysis on P_{set} and P_{reset} in the PF model. The left bar of each parameter represents the first-order SI and the right bar represents the total SI. As shown in Fig. 4(a), P_{set} is primarily controlled by r and D_β due to the higher total SIs, while the low first-order SIs suggest that their impact is largely due to interactions with other parameters. M_φ exhibits the highest first-order SI but the lowest total SI, indicating that its main effect is dominant, with minimal interaction effects with other parameters. Similarly, Fig. 4(b) illustrates the key parameters on P_{reset} . These key parameters are largely governed by the interactions, as the discrepancy between the total and the first-order SI is typically large. The impacts of M_φ , λ , and h are the most significant because their total SIs are greater than 0.5.

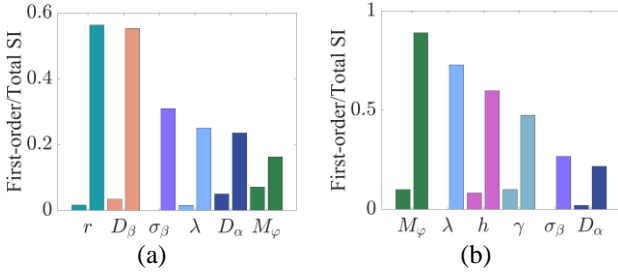


Figure 4: The results of the sensitivity analysis on (a) P_{set} and (b) P_{reset} in the PF model

Combining the results from the FE and PF models, the key parameters identified through UQ are inconsistent. This may be attributed to the differences in the physical processes concerned in the models: the FE model primarily focuses on a thermodynamic process, whereas the PF model concentrates on a kinetic process of microstructural evolution. In addition, both models suggest that electrical conductivity and thickness of the HfO_2 layer play a significant role. Finally, the results of two models complement each other and can provide a better understanding of the physical processes that occur in RRAM devices.

UQ on forming voltage

The forming voltage V_{forming} is an important performance index for RRAM. The KDE curve in Fig. 5 is derived from uncertainty propagation and shows the PDF of V_{forming} in the PF model. The KDE curve reveals the range of possible forming voltages and exhibits a bimodal distribution with two distinct peaks. The main peak is approximately located at 0.104 V, and the secondary peak appears near 0.078 V, suggesting two separate regions of high probability density for the forming voltage.

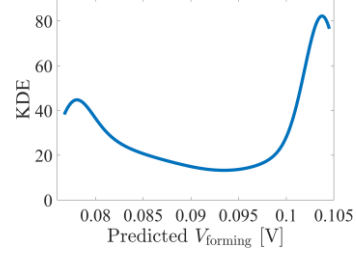


Figure 5: The KDE curve predicted by the uncertainty propagation on V_{forming} in the PF model

CONCLUSIONS

This work employed the UQ method to systematically analyze the impact of material uncertainty on the power consumption of RRAM in macroscopic FE model and mesoscopic PF model. By optimizing key parameters, the power consumption in the SET and RESET processes can be reduced by 32% and 38%, respectively. In addition, the study highlights the significant roles of electrical conductivity and the thickness of HfO_2 layer in both models. Furthermore, the probabilistic relationship between inputs and forming voltage is predicted. Future studies will investigate and quantify the uncertainty in RRAM performance at the atomic and electronic scales.

ACKNOWLEDGMENTS

This work was financially supported by the National Natural Science Foundation of China under grant number 51832002.

REFERENCES

- [1] D. Ielmini. *Semicond. Sci. Technol.*, vol. 31, 2016, pp. 063002-063026.
- [2] D. Niraula and V. Karpov. *J. Appl. Phys.*, vol. 124, 2018, p. 174502.
- [3] S. Kim, W. Kim, and T. Suzuki. *Phys. Rev. E*, vol. 60, 1999, pp. 7186-7197.
- [4] Y. Shibuta, Y. Okajima and T. Suzuki. *Scr. Mater.*, vol. 55, 2006, pp. 1095-1098.
- [5] M. Morris. *Technometrics*, vol. 33, 1991, pp. 161-174.
- [6] A. Saltelli and I. Sobol. *Reliab. Eng. Syst. Saf.*, vol. 50, 1995, pp. 225-239.
- [7] R. C. Smith. *Uncertainty Quantification: Theory, Implementation, and Applications*, SIAM, 2013.
- [8] B. Bichon, M. Eldred, L. Swiler, S. Mahadevan and J. McFarland. *AIAA J.*, vol. 46, 2008, pp. 2459-2468.